Janusz PODLIŃSKI[1], Katarzyna GARASZ[1], Artur BERENDT[1], Jerzy MIZERACZYK[2]

The Szewalski Institute of Fluid Flow Machinery, Polish Academy of Sciences, Fiszera 14, 80-231 Gdańsk, Poland (1)
Department of Marine Electronics, Gdynia Maritime University, Morska 81-87, 81-225 Gdynia, Poland (2)

doi:10.15199/48.2017.02.47

Electrohydrodynamic Flow Evolution in a Narrow Wire-Plate Electrostatic Precipitator

Abstract. *In this study, the temporal and spatial evolution of the electrohydrodynamic (EHD) flow for a high voltage positive pulse in a wire-plate electrostatic precipitator (ESP) is investigated, using the Time-Resolved Particle Image Velocimetry (PIV) method. The ESP consisted of a single wire electrode supplied by a positive high voltage and a two grounded plate electrodes. The images recorded just after applying the high voltage as well as velocity field maps of the EHD flow of the dust particles suspended in the air are presented. The results illustrate the temporal and spatial evolution of the EHD flow for different applied voltages and for cases without and with externally forced flow.*

Streszczenie. *W niniejszym artykule przedstawiono wyniki badań rozwoju przepływu elektrohydrodynamicznego (EHD) w elektrofiltrze z jedną drutową elektrodą wyładowczą zasilaną dodatnimi impulsami napięciowymi oraz z dwiema uziemionymi elektrodami płytowymi. Do badań wykorzystano czasowo-rozdzielczą metodę anemometrii obrazowej. Zaprezentowane wyniki ukazują rozwój przepływu EHD dla różnych napięć oraz dla przypadków bez i z wymuszonym przepływem (**Rozwój przepływu elektrohydrodynamicznego w wąskim elektrofiltrze typu drut-płyty**).*

Keywords: Electrostatic Precipitator, Electrohydrodynamic Flow, Temporal Flow Evolution, Time Resolved Particle Image Velocimetry.
Słowa kluczowe: Elektrofiltr, przepływ elektrohydrodynamiczny, rozwój przepływu w czasie, czasowo rozdzielcza metoda PIV.

Introduction

In the presence of the electric discharge, e.g. corona discharge or dielectric barrier discharge (DBD), the so-called ionic wind appears between the high voltage and grounded electrodes. The ionic wind sets the gas molecules and dust particles in motion and, as a consequence, an electrohydrodynamic (EHD) flow is formed. The interest of EHD flows has been rising, mostly due to its influence on the electrostatic precipitators (ESPs) performance [1-3] and the EHD flow potential to control the airflow around aerodynamic elements (e.g. airfoils) [4-7]. The subject of EHD flows behaviour in ESPs in the steady state (or time-averaged mode) has been undertaken and widely described by theoretical [e.g. 8-10] and experimental [e.g. 11-15] researchers. However, there is still a lack of knowledge in the area of the evolution of EHD flow in ESPs. It is not yet explained, how the ionic wind and EHD flow behave at the early stages, just after applying the high voltage to the discharge electrode or for the pulsed high voltage, which is increasingly used.

Some initial research on the time development of ionic wind and EHD flow in the wire-plate ESP was presented [16]. An interesting experimental results on the EHD flow evolution in a needle-to-plate corona discharge were also obtained [17, 18]. The results presented in [16-18] showed that during the unstable state of the discharge the EHD flow dramatically changes. One of the proposals to improve the collection efficiency of particles in ESPs is to use a new kind of power supply with combined DC and pulsed voltage. In such case electric field and corona discharge affected by the voltage pulses cause strong changes in the generated EHD flow, and, as one can suppose, the mechanism of dust particle collection is different than the one at the steady state (for DC high voltage). It is presently not clear, how this changes affect the overall collection efficiency of ESPs. We believe that temporal investigations of the EHD flow generated by the time-varying corona discharge with different parameters, could reveal some processes which are difficult to observe in other cases. Therefore, the study can be found very useful in providing a wider knowledge of the EHD phenomena occurring in devices, such as ESPs.

In this paper the images and flow velocity fields of the EHD flow evolution in a narrow ESP are presented. Narrow ESPs have become a subject of interest [19-22] because of their possible application for the cleaning of the exhaust gases emitted by diesel engines. In this work the ESP with a one discharge wire electrode and a two grounded plate electrodes was investigated. The EHD flow evolution was studied for three different values of the positive high voltage pulse applied to the wire electrode. The measurements were carried out without and with an externally forced flow.

Experimental setup

During the experiment, the temporal and spatial EHD flow structures generated by a corona discharge in the narrow wire-plate ESP were investigated. The flow images and vector velocity fields were registered using 2 Dimensional Time-Resolved Particle Image Velocimetry (2D TR PIV) method. The experimental setup (Fig. 1) consisted of the narrow wire-plate ESP, a high voltage power supply, a digital oscilloscope with a high-voltage probe and an ammeter, and a 2D TR PIV equipment.

The ESP electrode arrangement consisted of a three electrodes closed in a 500 mm x 120 mm x 50 mm acrylic box. The 0.9 mm in diameter stainless steel wire electrode was placed in the middle between the two plate electrodes, parallel to them, at 25 mm distance from each. The plate electrodes (500 mm long and 120 mm wide) were made of stainless steel. The positive high voltage was applied to the wire electrode through a 3.3 MΩ resistor. The plate electrodes were grounded.

High voltage applied to the wire electrode was measured with the oscilloscope Tektronics DPO 3034 and the discharge current was measured with the ammeter Brymen BM859CF. The current-voltage characteristics of the investigated wire-plate ESP for the DC positive voltage (at a steady state of voltage) are presented in Fig. 2. The measured corona onset voltage was about 14.5 kV.

The time-resolved measurements of the EHD flow evolution were taken for the early stage of the EHD flow occurring just after applying the DC high voltage to the discharge electrode. The measurements were carried out for a three different values of the DC voltage, i.e. amplitudes of a positive voltage pulse applied to the wire electrode: 16 kV, 18 kV and 20 kV. The time of appearing and pulse amplitude were remotely controlled by the digital function generator (Tektronix, AFG 3052C). The positive voltage pulse was generated by a high-voltage amplifier (TREK, 40/15). The rise time of the voltage pulse (from zero to the set value) was about 200 μs.

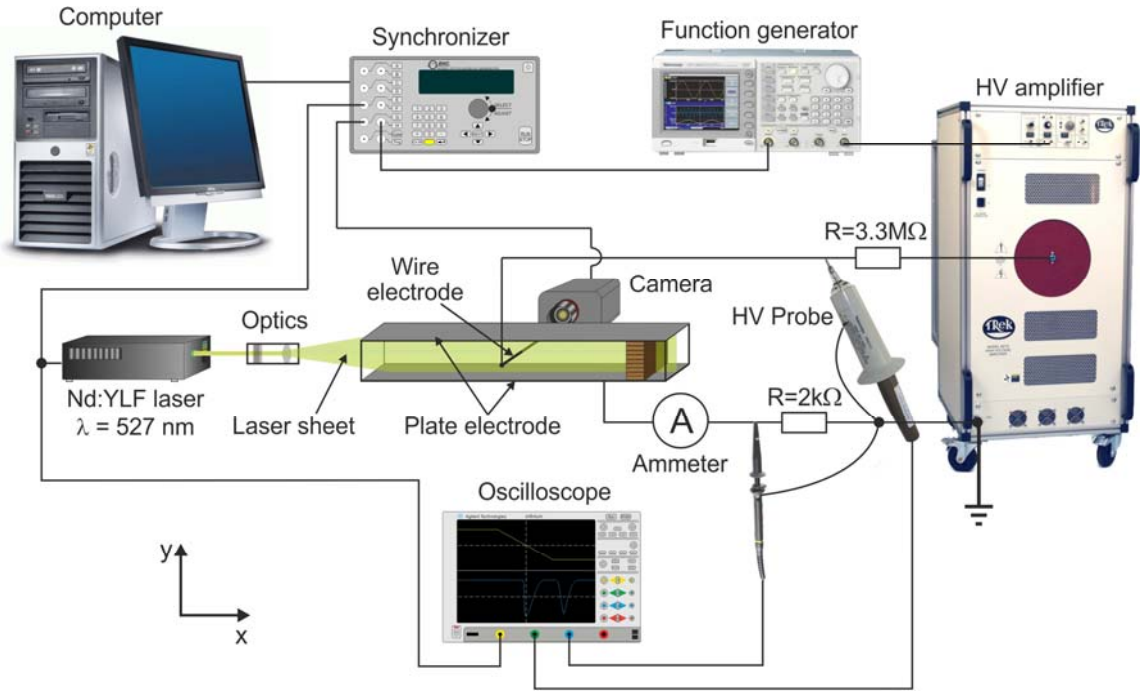

Fig.1. Experimental setup

The 2D TR PIV system used in this experiment was applied for both, the flow imaging and the measurement of flow velocity fields. It consisted of a twin Nd:YLF laser (Litron, 2 x 30 mJ at repetition rate 1000 Hz, 527 nm), an imaging optics (cylindrical telescope), a high speed CMOS camera (Phantom, Miro M340, camera sensor size 2560 × 1600 pixels), a digital signal generator (BNC, 575) for triggering the laser pulses and camera shutter, and a computer equipped with a Dantec DynamicStudio software for system controlling, recording the captured images and for digital analysis of the captured images. The diagram showing connections between the time-resolved measurement system devices is presented in Fig. 3.

The interior of the acrylic box with the wire-to-plate electrode arrangement was filled with air (at atmospheric pressure) seeded with a dust particles (incense smoke). The experiment was performed both, without and with externally forced flow through the ESP box. Before each measurement, the box was filled with a new seeded air, distributed with caution, to homogeneously fill the box volume. The initial dust concentration (before each measurement) only slightly varied during the investigations.

Results

Two kinds of the EHD flow studies are presented in this paper. The first one are images of particles suspended in the air which scatter the laser light. Every presented image was illuminated by only one laser pulse having duration of 150 ns, thus, every image can be treated as instantaneous. The second one are flow velocity fields. Every flow velocity field was calculated by the cross-correlation technique on the basis of two images recorder at an interval of 0.5 ms. The images and velocity field maps presented in this paper (Figs. 4-10) are selected to show the most representative results. Based on the measurements results, the evolution of the electrohydrodynamically-induced movement of suspended particles is described.

Figs. 4 and 5 show the evolution of the particle flow in the wire-plate ESP after applying the high voltage of 16 kV, when there was no externally forced flow. Just after (i.e. 75 μs) the voltage obtained the corona onset value (14.5 kV) the particles were distributed quite uniformly in the ESP (Fig. 4), as it was before applying the high voltage. No impact of the discharge was visible after such a short time. Only reflection of a laser light from the wire electrode (a small bright spot at xy (0,0)) and a shadow behind him (a dark line) can be observed.

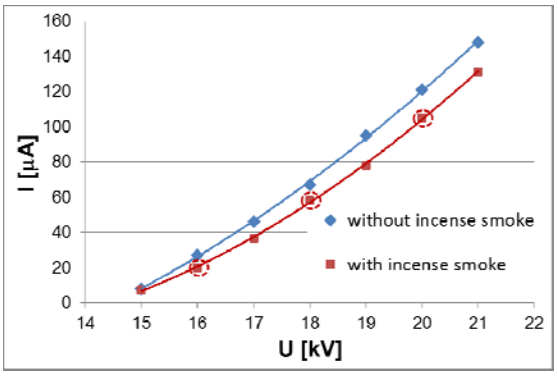

Fig.2. Current-voltage characteristics of the narrow wire-plate ESP for the DC positive voltage

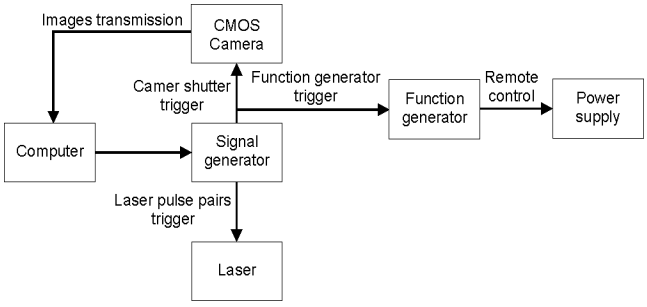

Fig.3. Block diagram of the time-resolved measurement system

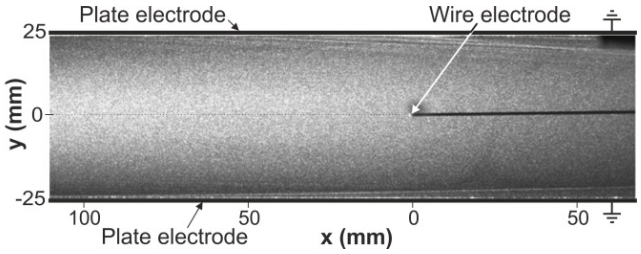

Fig.4. Image obtained in the narrow wire-plate ESP 75 μs after the corona discharge onset

The first disturbance of the quite uniform distribution of particles in the ESP was observed 0.5 ms after the corona onset (Fig. 5a). It was very tiny dark area in the form of a circle around the wire electrode. This dark area in the image means that the seeding particles have been removed from this area. At the first milliseconds after the corona discharge begins the dark area expanded, seeding particle removal from the close vicinity of the wire electrode can be observed (Figs. 5b-c). At 12.5 ms after the discharge onset, the seeding particles were forming a dark, regular circle free of particles, with the wire electrode in the middle. After about 30 ms, the circle still expanded and transformed into a bit oval shape (Fig. 5d). At about 50 ms (Fig. 5e), an asymmetrical ring around the central dark circle began to form. The ring then detached and expanded further towards the grounded electrodes. At about 120 ms after the corona onset (Fig. 5g), the distorted oval ring hit the grounded electrodes, which results in further formation of irregular vortices (Figs. 5h). The vortices formed quite symmetrical (to the axis line perpendicular to the plate electrode and passing through the wire electrode) structures. However, some asymmetry can be observed between top and bottom part of the ESP. Only a small vortex development can be observed near the bottom grounded plate and more developed vortices were formed near the upper grounded plate. This asymmetry suggests that the corona discharge to the top plate electrode was a bit stronger than to the bottom plate electrode. It could be caused by a small asymmetry in the wire electrode placement in between the plate electrodes. After about 355 ms (Fig. 5i) the irregular pattern of vortices filled 200 mm long area in between plate electrodes, while the distorted dark oval was still visible in the centre, around the wire electrode.

Fig. 6 shows a velocity vector maps of the EHD particle flow on the early stage of development after applying the positive voltage of 16 kV and without externally forced flow. The particles tendency to expand from the wire electrode in all directions is clearly visible. As one can see, the particles movement was detected in much wider area around the wire electrode then it could be observed on the presented images. For example, at 2.5 ms after the corona onset the dark circle had a diameter of 4 mm (Fig. 5b), while the vectors showing the particles movement form a circle with a diameter of about 18 mm (Fig. 6a). At 32.5 ms after the corona onset the dark circle observed on the image had about 20 mm (Fig. 5d), while the velocity vector map (Fig. 6c) clearly shows that the EHD flow occupied already whole area between plate electrodes (50 mm). On the other hand, in this case, in the circle having 20 mm diameter it was not possible to calculate velocity vectors because there were no particles. Similar pattern development of velocity vectors was obtained in the early stage for all investigated cases without externally forced flow, therefore, they are not presented in the paper.

In Figs. 7 and 8 the results for three different values of high voltage applied to the wire electrode are compared. Fig. 7 shows the patterns obtained at the early stage of the EHD particle flow evolution, i.e. 7.5 ms after the corona onset, while Fig. 8 shows the patterns at 52.5 ms after the corona onset. As one can suppose the dark circle pattern develops faster with the higher voltage applied. Moreover, in the later stage of development, the flow pattern forms more symmetrical structures between the top and bottom part of the ESP. It can be explained by a smaller influence of geometrical asymmetry at the higher voltage applied.

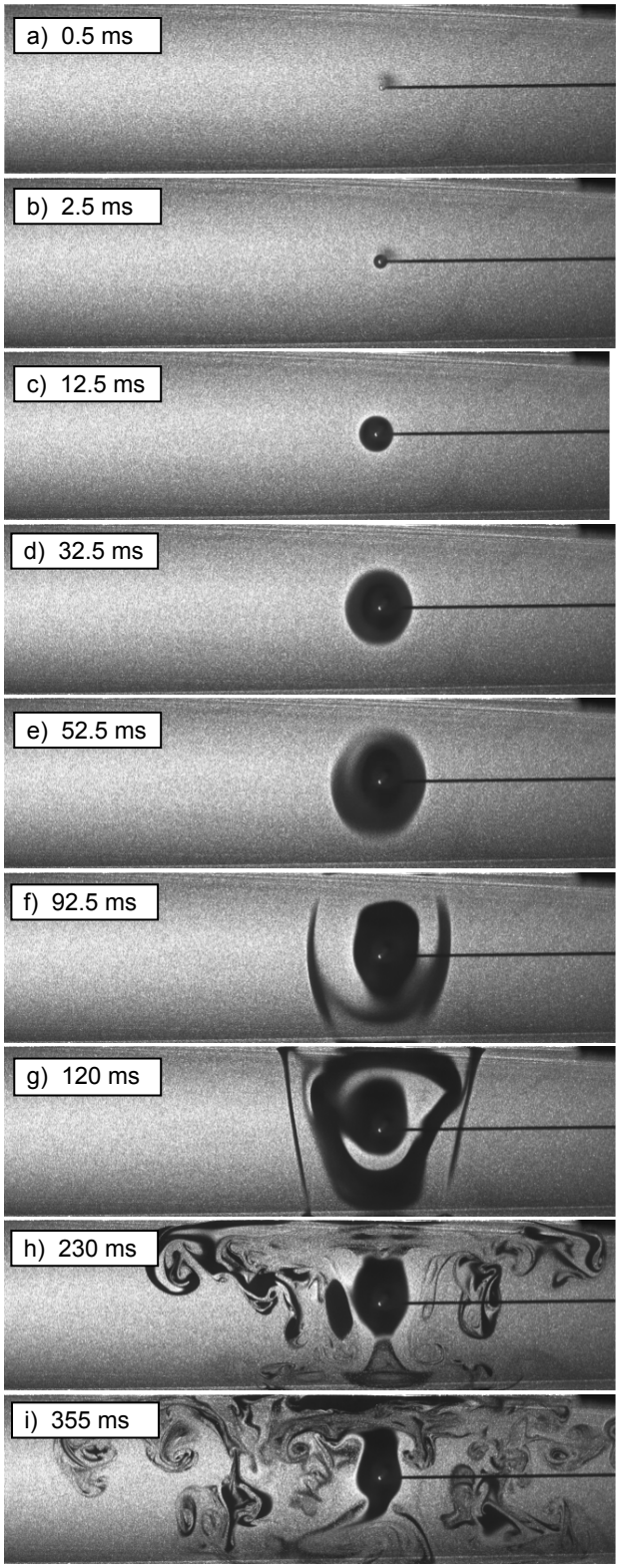

Fig.5. Images of the EHD flow evolution from 0.5 ms to 355 ms after the corona discharge onset in the wire-plate ESP. Positive voltage of 16 kV applied, without externally forced flow.

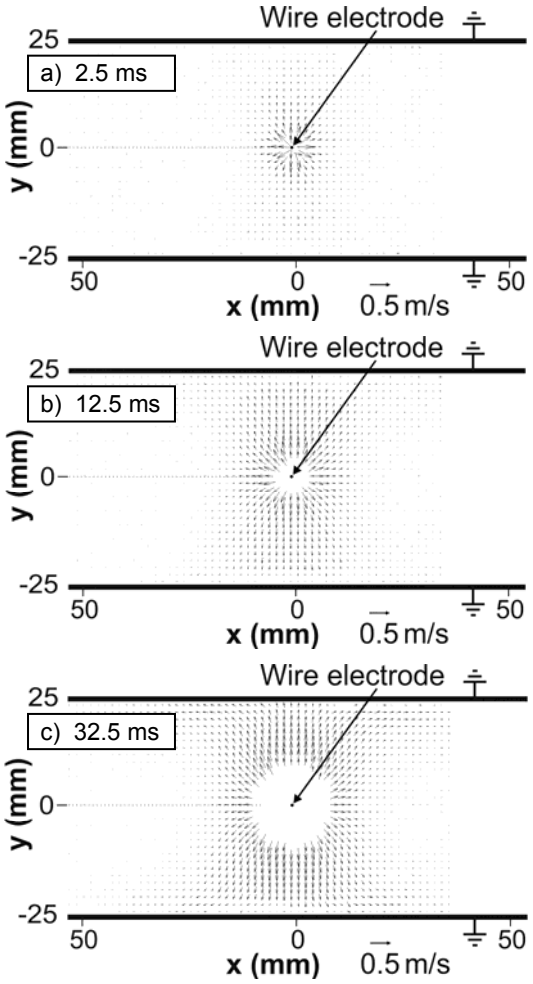

Fig.6. Vector fields of the EHD particle flow in the wire-plate ESP at: a) 2.5 ms, b) 12.5 ms, c) 32.5 ms after the corona discharge onset. Positive voltage of 16 kV applied, without externally forced flow.

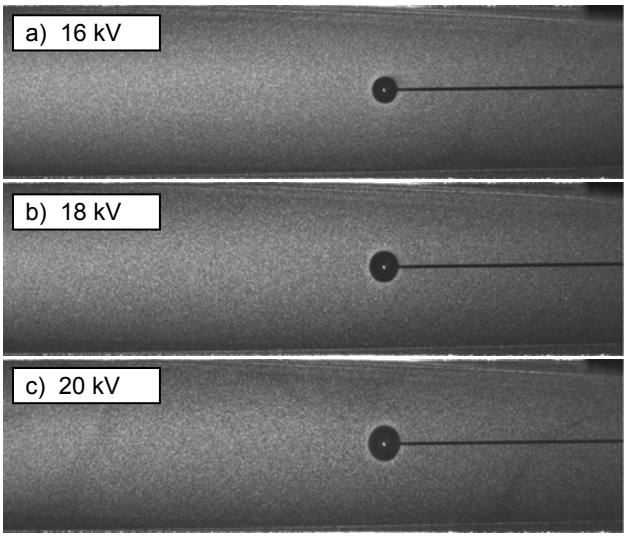

Fig.7. Images of the EHD flow evolution at 7.5 ms after the corona discharge onset in the wire-plate ESP. DC voltage of 16 kV, 18 kV or 20kV applied to the wire electrode, without externally forced flow.

Figs. 9 and 10 show the results obtained when there was externally forced flow in the ESP. Fig. 9 presents images of the EHD flow patterns at 7.5 ms after the corona discharge onset. At Fig. 9a the EHD flow pattern obtained for 0.4 m/s externally forced flow and 16 kV applied is presented. Fig. 9b shows results obtained at the same flow velocity (0.4 m/s), but for a higher voltage applied (18 kV). Fig. 9c shows results for a voltage of 18 kV and 0.8 m/s of externally forced flow.

All the cases presented in Figs. 9 and 10 differ from the previous results obtained without externally forced flow. The circular pattern around the wire electrode now is in a shape of a crescent. The dust particles were pushed away from the wire electrode in all directions (by electric force) and, at the same time, were entrained by the externally forced flow downstream the wire electrode. It results in a quite symmetrical structure between a top and bottom part of the ESP (due to the electric field and corona discharge symmetry), but asymmetrical structure in the externally forced flow direction (along the ESP). The characteristic shape of the dark area obtained downstream the wire electrode is caused by the flow trace behind the wire, where the velocity is significantly reduced.

As it can be seen in Figs. 9a and 9b the EHD flow pattern expanded faster towards the plate electrodes for higher voltage applied. It should be noticed that for the cases with externally forced flow of 0.4 m/s the dark pattern extended from the wire electrode to the plate electrodes as much as in the cases without external flow (compare Fig. 7a and Fig. 9a - the cases with 16 kV applied; as well as Fig. 7b and Fig. 9b - the cases with 18 kV applied).

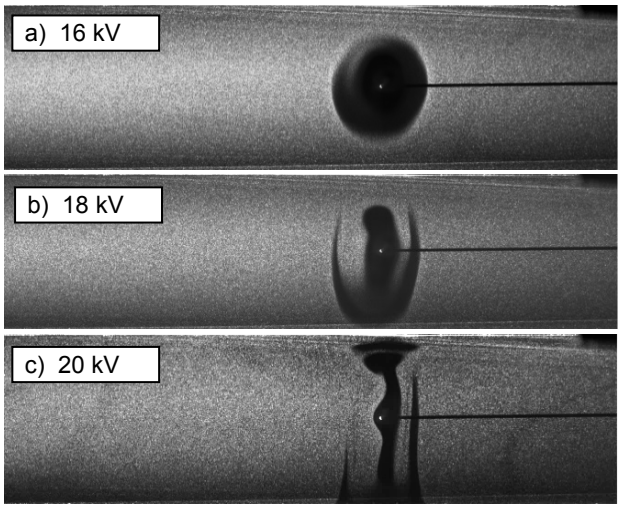

Fig.8. Images of the EHD flow evolution at 52.5 ms after the corona discharge onset in the wire-plate ESP. DC voltage of 16 kV, 18 kV or 20kV applied to the wire electrode, without externally forced flow.

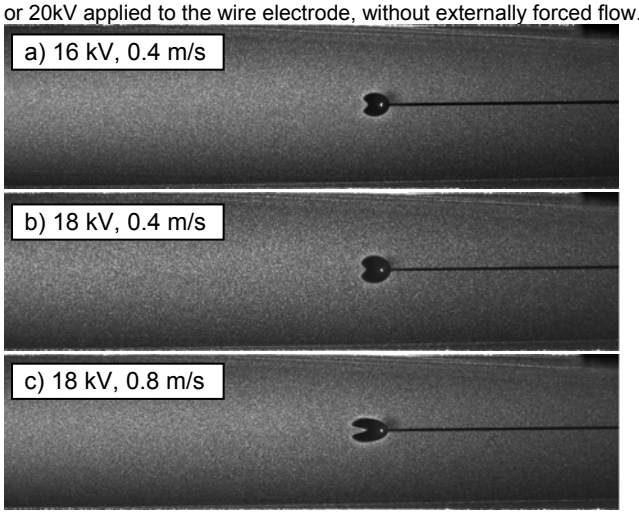

Fig.9. Images of the EHD flow evolution at 7.5 ms after the corona discharge onset in the wire-plate ESP. DC voltage of 16 kV or 18 kV applied to the wire electrode, externally forced flow of 0.4 m/s or 0.8 m/s.

The higher velocity of externally forced flow (0.8 m/s) caused faster extend of the EHD flow structure in x direction, i.e. along the ESP (Fig. 9c). However, in this case the dark area was narrower in the y direction (plate-to-plate) than it was in previous cases with the same applied voltage but with lower velocity of externally forced flow or without it. It suggests that for the externally forced flow of 0.8 m/s the particles were entrained from vicinity of the wire electrode before they were fully charged and moved by electrical force.

Fig. 10 shows results obtained 32.5 ms after the corona onset for the same applied voltages and externally forced flow velocities as it was presented in Fig. 9. All effects and dependencies which occured at the early stage of the EHD flow evolution (presented in Fig. 9) and describe above can be observed also in Fig. 10. Moreover, at the later stage of the EHD flow evolution some asymmetry caused by disturbances of externally forced flow emerging in the vicinity of the wire electrode are visible.

Conclusions

In this study, the temporal and spatial evolution of the EHD flow in the narrow wire-plate ESP for the high voltage positive pulse was investigated. In the cases without externally forced flow, just after applying the high voltage pulse, the pattern of the EHD particle flow follows the characteristic steps: the formation of a dark circle centred around the wire electrode, expansion of the dark circle from the wire electrode in all directions, formation and detachment of the higher velocity distorted ring around the circle, formation of the asymmetrical vortices when the ring meets the grounded plate electrodes.

The measured EHD flow patterns were slightly asymmetrical between the top and bottom part of the ESP, most probably because of some small geometrical asymmetry. Higher voltage applied to the wire electrode results in a faster evolution and improvement of symmetry of the EHD flow pattern generated by the discharge.

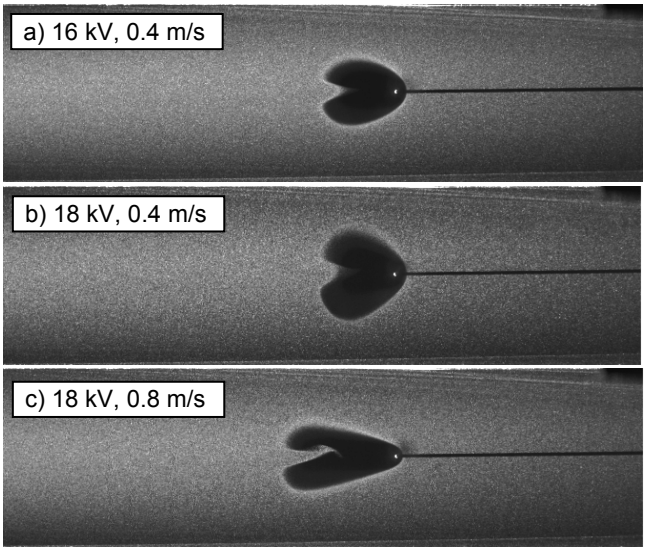

Fig.10. Images of the EHD flow evolution at 32.5 ms after the corona discharge onset in the wire-plate ESP. DC voltage of 16 kV or 18 kV applied to the wire electrode, externally forced flow of 0.4 m/s or 0.8 m/s.

In the cases with an externally forced flow the dark circle around the wire electrode transforms into an asymmetrical crescent like structure, expands towards the grounded plate electrodes and downstream the wire electrode. The expansion towards the plate electrodes depends on the velocity of externally forced flow and is lower for higher velocity. Moreover, disturbances of externally forced flow emerging in the vicinity of the wire cause asymmetry in the EHD flow pattern downstream the wire electrode. Depending on the velocity of externally forced flow the EHD flow pattern can evolve into various forms.

Acknowledgements

This work was supported by the research project no. 2014/13/D/ST8/03212 funded by the National Science Centre, Poland.

***Authors**: dr inż. Janusz Podliński, Instytut Maszyn Przepływowych im. Roberta Szewalskiego Polskiej Akademii Nauk, Ośrodek Techniki Plazmowej i Laserowej, ul. Fiszera 14, 80-231 Gdańsk, E-mail: janusz@imp.gda.pl; mgr inż. Katarzyna Garasz, Instytut Maszyn Przepływowych im. Roberta Szewalskiego Polskiej Akademii Nauk, Ośrodek Techniki Plazmowej i Laserowej, ul. Fiszera 14, 80-231 Gdańsk, E-mail: kgarasz@imp.gda.pl; mgr inż. Artur Berendt, Instytut Maszyn Przepływowych im. Roberta Szewalskiego Polskiej Akademii Nauk, Ośrodek Techniki Plazmowej i Laserowej, ul. Fiszera 14, 80-231 Gdańsk, E-mail: aberendt@imp.gda.pl; prof. dr hab. inż. Jerzy Mizeraczyk, Akademia Morska w Gdyni, Wydział Elektryczny, ul. Morska 81-87, 81-225 Gdynia, E-mail: jmiz@imp.gda.pl.*

REFERENCES

[1] Masuda S., Hosokawa S., Chapter 21 of Handbook of electrostatic processes, Marcel Dekker, NY 1995, pp. 441-479
[2] Mizuno A., IEEE Trans. Diel. Electr. Insul., 7, (2000), pp. 615-624
[3] Mizeraczyk J., Podlinski J., Niewulis A., Berendt A., J. Phys. Conf. Ser., 418, (2013), 012068
[4] Moreau E., J. Phys. D: Applied Physics, 40, (2007), pp. 605-636
[5] Touchard G., IJ PEST, 2, (2008), pp. 1 25
[6] Berendt A., Podlinski J., Mizeraczyk J., Eur. Phys. J. Appl. Phys., 55, (2011), 13804
[7] Berendt A., Podlinski J., Mizeraczyk J., Przeglad elektrotechniczny, 88, 8, (2012), pp. 18–21
[8] Brocilo D., Chang J.S., Findlay R.D., in Proc. 8th Int. Conf. on Electrostatic Precipitation, Birmingham, USA, (2001), pp. 1–18
[9] Yamamoto Y., Okuda M., Okubo M., IEEE Trans. Ind. Appl. 39 (2002), pp. 1602–1607
[10] Farnoosh N., Adamiak K., Castle G.S.P., J. Electrostat. 69, (2011), pp. 419-428
[11] Yamamoto T., Velkoff H.R., J. Fluid Mech., 108, (1981), pp. 1-18
[12] Jędrusik M., Gajewski J.B., Świerczok A.J., J. Electrostat. 51-52, (2001), pp. 245–251
[13] Chang J.S., Dekowski J., Podlinski J., Brocilo D., Urashima K., Mizeraczyk J., IEEE Industry Applications Conference, Book Series: IEEE Industry Applications Society Annual Meeting, Vol 4, (2005), pp. 2597-2600
[14] Podlinski J., Berendt A., Mizeraczyk J., IEEE Trans. Dielectr. Electr. Insul., 20, 5, (2013), pp. 1481-1488
[15] Zhiyuan N., Podlinski J., Xinjun S., Shuran L., Shilong W., Ping H., Keping Y., J. Electrostat. 80, (2016), pp. 76-84
[16] Mizeraczyk J., Dekowski J., Podlinski J., Kocik M., Ohkubo T., Kanazawa S., J. Visualization, 6, 2, (2003), pp. 125-133
[17] Tanoue K-I., Taniguchi H., Masuda H., Advanced Powder Technol., 17, (2006), 69-83
[18] Mizeraczyk J., Berendt A., Podlinski J., J. Phys. D: Applied Physics, 49, 20, (2016), 205203
[19] Niewulis A., Podlinski J., Kocik M., Barbucha R., Mizeraczyk J., Mizuno A., J. Electrostat., 65, (2007), pp. 728-734
[20] Boichot R., Bernis A., Gonze E., J. Electrostat., 66, (2008), pp. 235–245.
[21] Yamamoto T., Mimura T., Otsuka N., Ito Y., Ehara Y., Zukeran A., IEEE Trans. Ind. Appl., 46, (2010), pp. 1606–1612.
[22] Niewulis A., Berendt A., Podlinski J., Mizeraczyk J., J. Electrostat., 71, (2013), pp. 808-814